Cite this article
Fantilli AP and Jóźwiak-Niedźwiedzka D
Influence of Portland cement alkalinity on wool-reinforced mortar.
Proceedings of the Institution of Civil Engineers – Construction Materials,
https://doi.org/10.1680/jcoma.20.00003

Research Article
Paper 2000003
Received 30/12/2019;
Accepted 15/06/2020

Keywords: fibre-reinforcement/microstructure/waste valorization

Construction Materials

ice Publishing

Influence of Portland cement alkalinity on wool-reinforced mortar

Alessandro P. Fantilli PhD, MSc
Associate Professor, Department of Structural, Geotechnical, and Building Engineering, Politecnico di Torino, Torino, Italy (corresponding author: alessandro.fantilli@polito.it) (Orcid:0000-0003-0383-7191)

Daria Jóźwiak-Niedźwiedzka PhD, DSc, CE
Assistant Professor, Institute of Fundamental Technological Research, Polish Academy of Sciences, Warsaw, Poland
(Orcid:0000-0003-3681-0817)

Natural wool is a good insulating material, both thermally and acoustically. With the increase in demand for the usage of waste materials, other applications have been found, such as the use of wool as a fibre reinforcement in mortars and concretes. Unfortunately, wool, like other natural organic materials, dissolves in alkaline environments and, consequently, the performance of wool reinforcement cannot be guaranteed for a long time. To address this issue, three series of wool-reinforced mortar beams, with various contents of alkalis in cement, were investigated. The chemical compatibility and the effects of alkalinity on mechanical performance were investigated by testing the beams under three-point bending and, subsequently, by analysing the microstructure of the mortars using energy-dispersive X-ray spectroscopy. The results showed that the lower the alkalinity of the cement paste, the better the resistance of wool fibres in the cementitious matrix, thus guaranteeing larger post-cracking residual stresses in the wool-reinforced mortars.

Notation

A_F	area defined by x–y curve (flexural toughness)
P	applied load in three-point bending test
P_{max}	maximum applied load in three-point bending test
x	difference δ–δ_p (for $\delta \geq \delta_p$)
y	ratio P/P_{max}
δ	mid-span deflection of beam in three-point bending test
δ_p	mid-span deflection of beam at P_{max}

1. Introduction

Many studies have been carried out on cement-matrix composites modified with various cementitious supplementary materials (e.g. fly ash, silica fume, ground-granulated blast furnace slag) and reinforced with traditional fibres such as steel, glass, carbon or basalt (Fantilli *et al.*, 2011; Jena *et al.*, 2018; Jóźwiak-Niedźwiedzka *et al.*, 2012; Ralegaonkar *et al.*, 2019). Due to the relatively high cost of manufactured fibres and the negative influence of their industrial production on the environment, natural fibres (e.g. wool) are frequently proposed as potential alternatives. The use of natural fibres as reinforcement in cement-based composites can increase the toughness of concretes and mortars, while also being sustainable alternative to traditional industrial fibres. Such fibres can bridge the surfaces of the cracks in the post-cracking stages and reduce the environmental impact of the construction industry (Fantilli *et al.*, 2017a).

Natural wool is one of the earth's most sustainable fibres, as it is a resource constantly produced over time. It is also an environmentally-friendly material, because it is easily recycled and biodegradable. In addition, existing sheep's wool in Europe is not suitable for the textile industry (Štirmer *et al.* 2014) and the amount of unused wool is around 150 Mt/year, to which the wool contained in other end-of-life products (e.g. fitted carpets) and in textile industry wastes have to be added (Schokker, 2010). This unused wool is nowadays considered as special waste, which needs sterilisation treatment (at 130°C) before its disposal. Looking for a possible application of these fibres, also in alternative to other natural fibres (such as hemp – see Fantilli *et al.*, 2017a), is therefore of paramount importance. Research studies on the applications of sheep's wool in the construction industry are mainly related to using it as an insulating material, both thermal and acoustic. Very few studies have been reported on wool as a reinforcement material in cement-based composites (see, for example, the characterisation of cementitious mortars with multifunctional addition of unused wool fibres carried out by Jóźwiak-Niedźwiedzka and Fantilli (2017)). This is mainly due to durability reasons.

The alkalinity of cementitious matrices significantly damages both vegetal and animal fibres, which can completely degrade over time (Fantilli *et al.*, 2017b; Tolêdo Filho *et al.*, 2000). In the case of vegetal fibres, their reduced durability is associated with a reduced pullout strength because alkaline-induced degradation reduces the cross-sectional area of the fibres. In fact, the change of volume produced by water absorption and the migration of hydration products, especially calcium hydroxide, to the fibre lumen, walls and voids, drastically reduce the bond between the fibres and the matrix (Tolêdo Filho *et al.*, 2000). However, the principal mechanisms

that produce the degradation of vegetal fibres are summarised as follows.

- Peeling-off phenomenon produced by alkaline water contained in the micropores of the cementitious matrix. This water can dissolve the lignin and hemicellulose existing in the middle lamellae of the fibres and weakens the links between the cellulose of the fibres (Tolêdo Filho *et al.*, 2000).
- Alkaline hydrolysis of the cellulose molecules produces degradation of the molecular chains and a reduction in both the degree of polymerisation and tensile strength (Wei and Meyer, 2014).

To mitigate the degradation of vegetal fibres used as reinforcement in cement-based mortars and concretes, either a special treatment of the fibres or modification of the cementitious matrix needs to be adopted. Chemical or physical methods are frequently used to improve the performance of such fibres. Wei and Meyer (2014) showed that both acrylic emulsion and alkylalkoxysilane surface treatments of natural fibres provided better durability properties and higher bending strengths of the fibre-reinforced composites. Moreover, the effectiveness of vegetal fibre reinforcement in cementitious matrices can be improved by adding supplementary cementitious materials to the common concrete and mortar components. In some cases, the partial substitution of Portland cement with fly ash or silica fume can reduce the alkalinity of the cementitious matrix and, consequently, the degradation of the vegetal fibres. Positive results have been obtained by mixing sisal or coconut fibres with silica fume before adding them to a cementitious matrix (Tolêdo Filho *et al.*, 2000).

Although there are extensive research activities on the use of vegetal fibres as reinforcement for cement-based composites, studies on the compatibility of animal fibres and cementitious matrices are very scarce in the literature. In particular, a direct correlation between the durability of wool and the mechanical performance of wool-reinforced composite is desirable. Some researchers have showed that, with the addition of sheep's wool, density and thermal insulation improved but, at the same time, the mechanical properties of the composite decreased (Štirmer *et al.* 2014). Fiore *et al.* (2019) studied the mechanical behaviour and thermal conductivity of a cement mortar with various lengths and different contents (13%, 23% and 46% by weight of cement) of wool fibres. They found that the wool-reinforced composites showed lower compressive strength than the reference no-wool cement composite, regardless of the content or length of fibres. These trends did not change when fly ashes were added to concrete mixtures reinforced with sheep's wool fibres (Grădinaru *et al.*, 2016). In addition, wool fibres pre-treated with atmospheric plasma did not improve the performance of the mortars (Fantilli *et al.*, 2017a).

Wool is a natural material and the long-term effects of its use in cement-based materials should be considered in terms of durability. However, very limited data can be found in the literature. Giosué *et al.* (2019) noted an increase of 30% in total open porosity in hydraulic lime mortars containing 25% of wool fibre when compared with a reference mortar without fibres. Pederneiras *et al.* (2019) attributed this increment to the fibre–matrix interface, which is less compact than in the case of a sand–cement matrix. Recently, Allafi *et al.* (2020) presented a review of the advancements in applications of natural wool fibre. However, in all of the above publications, there is no information on the durability of cement-based composites with the addition of wool fibres.

Table 1. Chemical composition of cement determined by X-ray fluorescence (wt%)

Constituent	L – low-alkali cement	N – normal cement	H – high-alkali cement
Silicon dioxide	20.82	19.03	19.43
Aluminium oxide	4.41	4.84	4.84
Ferric oxide	5.34	3.22	3.18
Calcium oxide	63.31	63.64	61.81
Magnesium oxide	0.93	1.15	2.56
Sulfur trioxide	2.57	2.97	3.93
Sodium oxide	0.28	0.21	0.41
Potassium oxide	0.25	0.53	1.08
Sodium oxide equivalent	0.44	0.56	1.12

Figure 1. Sheep's wool used to reinforce cement-based mortars

Table 2. Composition and curing conditions of the analysed mortars

Series	Type of cement	Wool content: g	Time and curing conditions
N_1	N	—	27 days in room conditions (20°C, RH = 50%)
N_2	N	10	27 days in room conditions (20°C, RH = 50%)
N_3	N	10	27 days in water (20°C)
N_4	N	10	3 days in water (20°C)
L_1	L	—	27 days in room conditions (20°C, RH = 50%)
L_2	L	10	27 days in room conditions (20°C, RH = 50%)
L_3	L	10	27 days in water (20°C)
L_4	L	10	3 days in water (20°C)
H_1	H	—	27 days in room conditions (20°C, RH = 50%)
H_2	H	10	27 days in room conditions (20°C, RH = 50%)
H_3	H	10	27 days in water (20°C)
H_4	H	10	3 days in water (20°C)

Thus, in this work, new tests were carried out with the aim of modifying the alkalinity of cement-based matrices. Specifically, this work investigated the mechanical properties (e.g. flexural strength) of wool-reinforced mortars made with different Portland cements and their microstructures. The results of the tests are reported and discussed in this paper.

2. Materials and methods

2.1 Materials

Standard natural siliceous sand, with a size distribution within the limits given by BS EN 196-1:2005 (BSI, 2005) (specific gravity of 2.65 g/cm^3 and maximum grain size of 2 mm), and tap water were used to prepare the mortar. Three different Portland cements (CEM I 42.5R) with different alkali contents (N – normal cement with a sodium oxide equivalent $(Na_2O)_{eq}$ of 0.6%, H – high-alkali cement with a sodium oxide equivalent of 1.1% and L – low-alkali cement with a sodium oxide equivalent of 0.4%) were used. The chemical compositions of these cements are provided in Table 1. Wool fibres with a density of 1.0 g/cm^3 (Figure 1) were used in the amount of 1% by volume. The geometrical properties of wool vary, but 19 μm and 16 mm are, respectively, the average diameter and the average length of the filaments (Fantilli *et al.*, 2017a; Jóźwiak-Niedźwiedzka and Fantilli, 2017). Their tensile strength is about 240 MPa, as measured with a testing machine equipped with a loading cell of 10 N (displacement rate = 0.05 mm/s).

2.2 Mixing and proportioning

Three series of mortars, classified in Table 2 on the base of the type of cement, were designed and tested. Each series included four different batches, depending on the curing conditions. From each batch, three prismatic specimens $40 \times 40 \times 160$ mm were fabricated for bending tests (a total of 36 specimens). They remained in the moulds for 1 day at room conditions (20°C, relative humidity (RH) = 50%). After demoulding, and before the tests, the specimens of series H_1, L_1, N_1, H_2, L_2 and N_2 were cured in the same room conditions for 27 days. On the contrary, the specimens of series H_3, L_3 and N_3 were left in water for 27 days and those of series H_4, L_4 and N_4 remained in water for only 3 days. The temperature of water was constant and equal to 20°C. In each batch, the mix proportion remained the same (i.e. 580 kg/m^3 of cement, 290 kg/m^3 of water and 1760 kg/m^3 of sand), as prescribed by BS EN 196-1:2005 (BSI, 2005).

2.3 Mechanical properties and microstructure analysis

The experimental tests were carried out in accordance with by BS EN 196-1:2005 (BSI, 2005). All the specimens were tested in three-point bending (see Figure 2) 28 days after casting, with the exception of specimens H_4, L_4 and N_4, which were

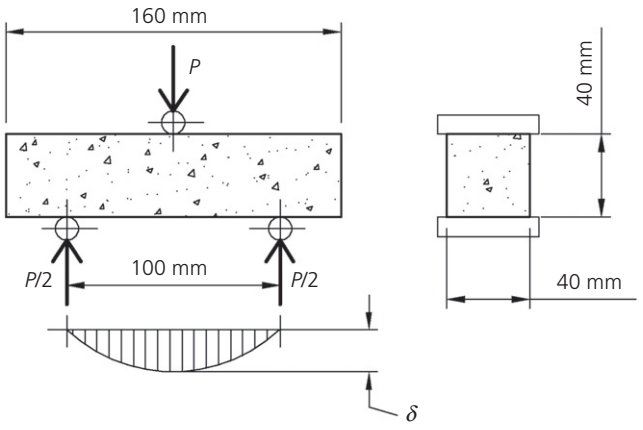

Figure 2. Three-point bending tests for cementitious mortars (BSI, 2005)

tested 4 days after casting. The external load P was applied at the mid-span of the specimens through a loading machine with a load capacity of 100 kN. Tests were performed by driving the displacement of the loading cell, whose stroke moved at a velocity of 0.05 mm/min.

Microstructural analysis was performed on the fractured surfaces of the mortar beams. A piece of mortar was mounted on a metal sample holder with the fracture surface of interest facing upwards and secured with a mixture adhesive and carbon tape. A conductive tape was traced along the periphery of the specimen, resting on the holder to improve the conductivity of the whole specimen assembly. The specimens were subsequently coated with a layer of carbon and thoroughly examined using SEM-EDX (scanning electron microscopy with energy-dispersive X-ray spectroscopy) by means of a Jeol

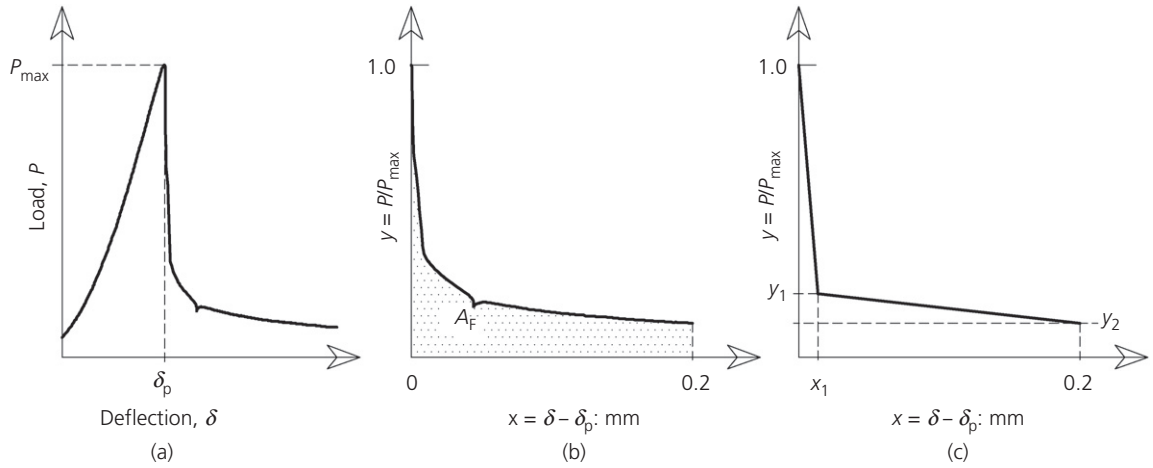

Figure 3. Results of three-point bending tests: (a) whole P–δ diagram; (b) post-peak behaviour; (c) bilinear relationship used to quantify the effect of fibres

Table 3. Main results of the three-point bending tests

	N_1			**N_2**			**N_3**			**N_4**		
P_{max}: kN	3.20	2.94	3.21	2.83	2.88	2.78	2.69	2.32	2.54	2.07	2.10	2.14
δ_p: mm	0.44	0.54	0.44	0.37	0.28	0.35	0.51	0.36	0.48	0.44	0.41	0.50
x_1: mm	0.02	0.01	0.03	0.02	0.02	0.02	0.03	0.03	0.02	0.02	0.02	0.02
y_1	0.01	0.00	0.00	0.09	0.09	0.10	0.02	0.02	0.07	0.12	0.11	0.05
y_2	0.01	0.00	0.00	0.03	0.04	0.04	0.01	0.01	0.01	0.04	0.04	0.02
A_F: mm	0.01	0.01	0.02	0.02	0.02	0.02	0.02	0.02	0.02	0.025	0.024	0.016
	L_1			**L_2**			**L_3**			**L_4**		
P_{max}: kN	2.59	2.31	2.58	1.90	1.76	1.69	2.35	2.19	2.35	1.44	1.60	1.43
δ_p: mm	0.56	0.43	0.48	0.52	0.78	0.65	0.51	0.39	0.74	0.35	0.41	0.38
x_1: mm	0.02	0.02	0.02	0.03	0.02	0.09	0.02	0.02	0.03	0.02	0.02	0.02
y_1	0.02	0.05	0.04	0.28	0.30	0.42	0.05	0.05	0.05	0.12	0.15	0.17
y_2	0.01	0.01	0.01	0.12	0.12	0.20	0.02	0.01	0.02	0.07	0.11	0.10
A_F: mm	0.01	0.02	0.01	0.05	0.05	0.10	0.02	0.02	0.02	0.03	0.03	0.03
	H_1			**H_2**			**H_3**			**H_4**		
P_{max}: kN	3.34	3.38	3.58	3.25	3.42	3.33	2.83	2.80	2.96	2.20	2.46	2.53
δ_p: mm	0.56	0.33	0.45	0.41	0.47	0.52	1.11	0.50	0.56	0.45	0.32	0.44
x_1: mm	0.01	0.02	0.03	0.03	0.03	0.03	0.02	0.03	0.03	0.03	0.02	0.02
y_1	0.01	0.01	0.01	0.03	0.05	0.04	0.03	0.03	0.02	0.03	0.06	0.06
y_2	0.00	0.00	0.00	0.02	0.03	0.02	0.00	0.01	0.01	0.01	0.02	0.02
A_F: mm	0.01	0.01	0.01	0.02	0.02	0.02	0.01	0.02	0.02	0.02	0.02	0.02

JSM-6380 LA personal scanning electron microscope in secondary electron mode, using an acceleration voltage of 15 kV.

3. Rest results

The three-point bending tests provided load–mid-span deflection diagrams similar to that shown in Figure 3(a). Important data were obtained from these P–δ curves. In particular, as illustrated in Figure 3(a), both the flexural strength, P_{max}, and the corresponding displacement, δ_p, were measured for all 36 tests.

As fibre reinforcement works in the post-cracking stage, a new approach was proposed to quantify the effect of the fibre reinforcement (Fantilli *et al.*, 2017a). Starting from the P–δ curves depicted in Figure 3(a), the new post-peak diagrams shown in Figure 3(b) were defined. The values of the normalised load ($y = P/P_{max}$) are reported on the ordinate and the difference x between the post-peak deflection and δ_p is on the abscissa of these diagrams. All the post-peak diagrams were limited to $x = 0.2$ mm in correspondence of which the residual load of the plain mortars was nearly zero. The flexural toughness of the mortars investigated could also be quantified by calculating the area A_F delimited by the post-peak curves (see Figure 3(b)).

To facilitate analysis of the results, a further simplification is introduced. In general, the post-peak curve depicted in Figure 3(b) can be approximated by a bilinear relationship (see Figure 3(c)). Thus, the most relevant data from the pre-peak stage is P_{max} (i.e. the strength of the mortar) and the corresponding deflection δ_p, whereas the residual stress of the post-cracking stage can be evidenced by A_F and the coordinates $[x_1, y_1]$ and [0.2 mm, y_2]. The values of all these parameters measured in the 36 specimens tested in three-point bending are reported in Table 3.

In Table 3, the values of A_F, which represents the overall capacity of the fibre to bridge the crack surfaces, can be computed through the formula:

$$A_F = \frac{1 + y_1}{2} x_1 + \frac{y_1 + y_2}{2}(0.2 - x_1) \quad (1)$$

where y_1 is the percentage of residual load just after cracking, y_2 is the percentage of residual load in the presence of large cracks and x_1 is the abscissa (in mm) in correspondence of y_1.

As shown in Table 3, the highest values of P_{max} were obtained for the reference mortars without the addition of fibres.

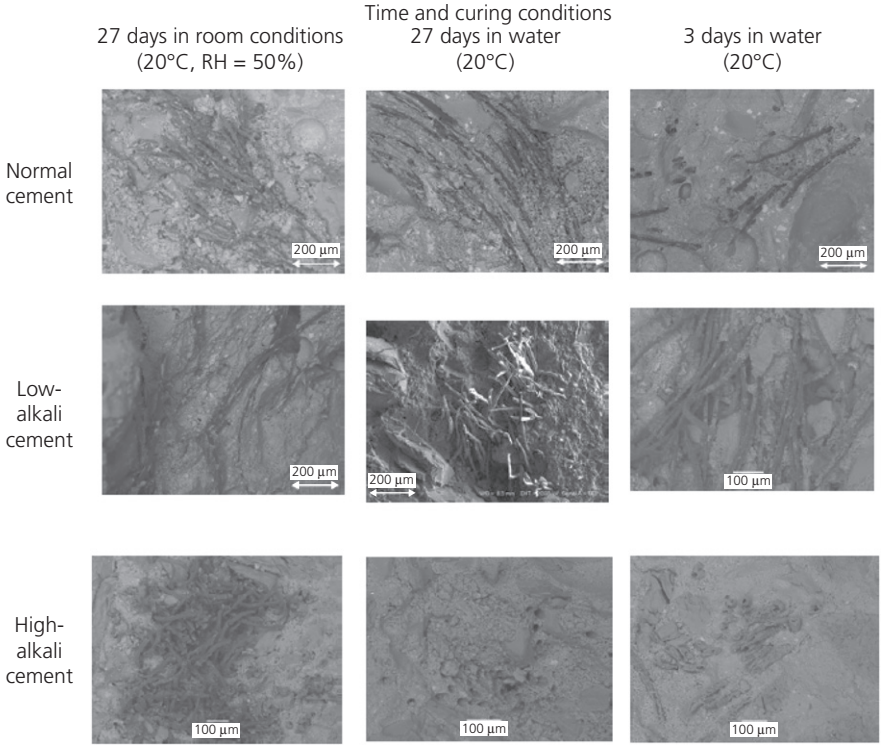

Figure 4. SEM images of the analysed mortars

However, the specimens made with the high-alkali cement, stored in the same room conditions and reinforced with fibres (series H_2) were characterised by similar P_{max} values. The curing time in water significantly influenced P_{max}. The longer the specimens were stored in water, the higher P_{max} regardless of the cement used.

Obviously, the larger the benefit of the fibre, the larger the value of y_1. The capacity for maintaining residual stress increased with A_F (and y_2). Both these mechanical parameters are strictly connected to the dissolution of wool at high pH values. Thus, the results of the three-point bending tests reported in Table 3 should be correlated with the SEM images of the fracture surfaces, taken after the bending tests. Micrographs of nine mortars reinforced with wool are shown in Figure 4. It can be observed that the higher the alkali content of the cement and the longer the curing time in water, the higher the degree of degradation of wool fibres (in Figure 4) and the lower the values of y_1 and A_F (in Table 3). The empty spaces shown in Figure 4, created after wool dissolution, produced the decrement in the mechanical properties of the wool-reinforced mortars.

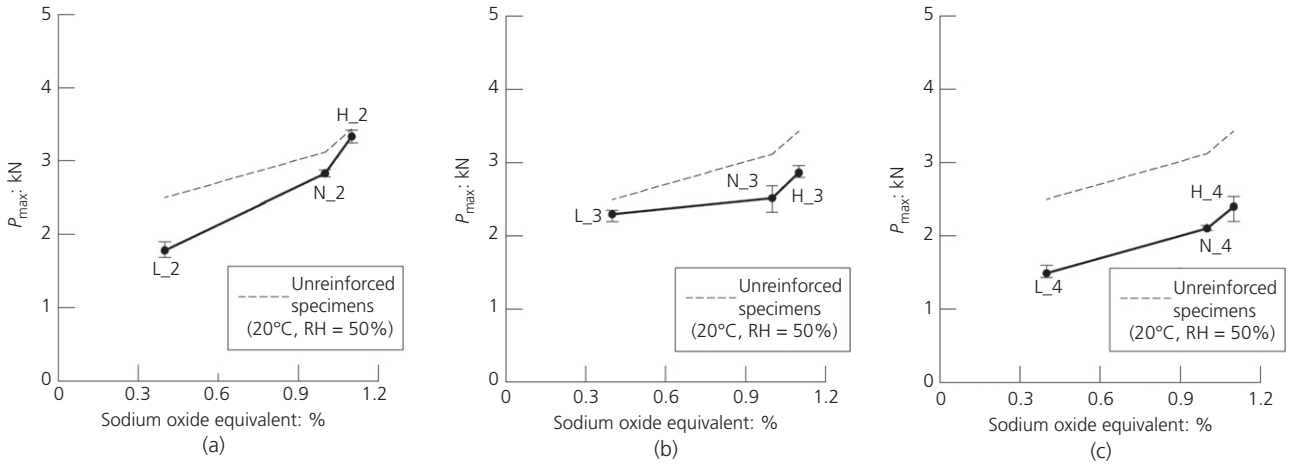

Figure 5. Flexural strength P_{max} measured in the three-point bending tests: (a) specimens cured for 27 days in room conditions (20°C, RH = 50%); (b) specimens cured for 27 days in water (20°C); (c) specimens cured for 3 days in water (20°C)

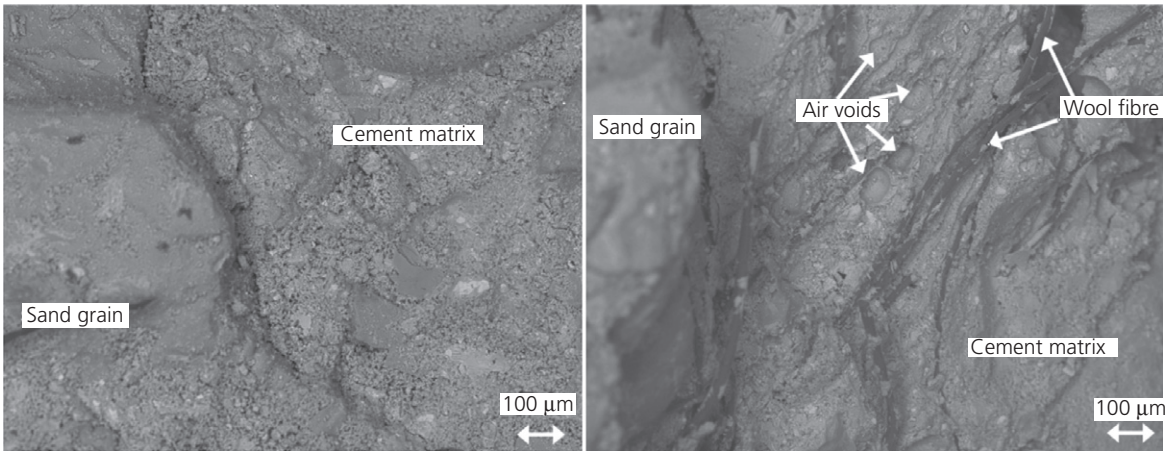

Figure 6. Microstructure of specimens made with low-alkali cement after 27 days of curing in 20°C and 50% RH (scale bar – 100 μm): (a) reference specimen L_1; (b) specimen with addition of wool fibres L_2

4. Analysis of results

The average values of P_{max} are reported in Figure 5(a) as a function of the alkalinity of cements. In this and subsequent diagrams, the values measured in unreinforced specimens (dashed lines) are assumed to be the reference. It is possible to observe that, for the room curing conditions (27 days at 20°C and RH = 50%), the lowest flexural strength was measured for the specimens made with the low-alkali cement, with and without fibre reinforcement (see Figure 5(a)). As the sodium oxide equivalent of the cement increased, the flexural strength also increased, and the maximum value been measured for the case of the high-alkali cement.

The increase in strength with the alkalinity showed more or less the same trend regardless of the content of fibres. Nevertheless, for the same type of cement, P_{max} decreased in the presence of fibres due to the reduction of both workability and density of the mortar. Indeed, the fibre-reinforced matrix contained more voids, as illustrated in Figure 6, where SEM images of plain mortar (Figure 6(a)) and wool-reinforced mortar (Figure 6(b)) are compared in the case of the low-alkali cement.

After curing in water for 27 days at 20°C, the P_{max} value increased with an increase of sodium oxide equivalent content (see Figure 5(b)), although it was not visible in the case of standard curing conditions shown in Figure 5(a). In other words, as the sodium oxide equivalent increased, the difference in strength, with respect to plain mortars cured for 27 days at 20°C and RH = 50%, increased. The same trend can also be observed in Figure 5(c), where data related to the wool-

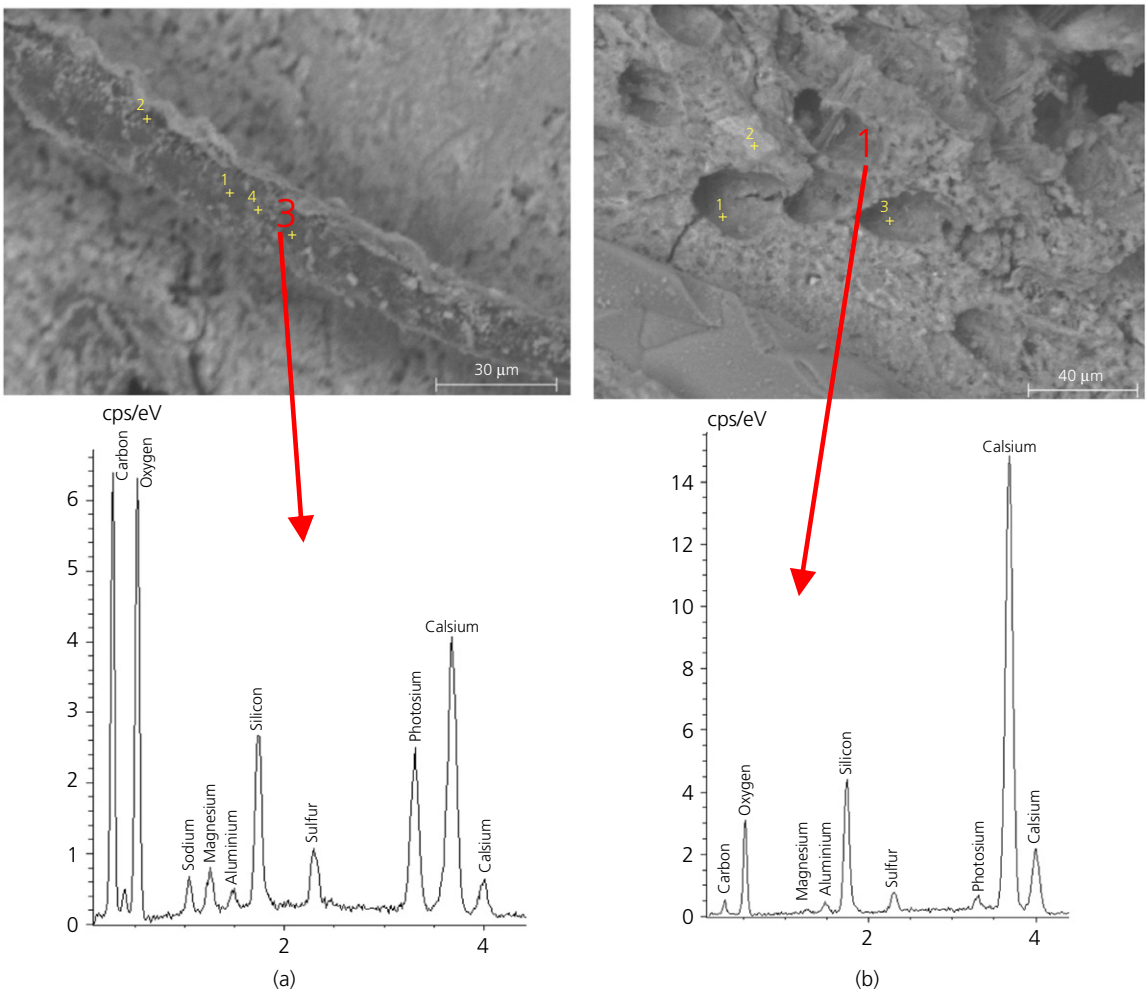

Figure 7. Microstructure of specimens made with high-alkali cement and reinforced with wool fibres with EDX analysis in microareas: (a) H_4 – after 3 days of curing in water at 20°C (analysis in the microarea on wool fiber); (b) H_3 – after 27 days of curing in water at 20°C (microarea analysis in a matrix after a degraded wool fiber)

reinforced specimens left for only 3 days in water (at 20°C) are reported. In all the cases, the flexural strength of the mortars containing fibres was lower than that of plain mortar cured for 28 days at 20°C and RH = 50%.

This reduction in strength can be ascribed to the degradation of the wool fibres, which seems to affect the cementitious matrix also. The empty holes due to wool fibre dissolution were particularly visible in the mortar specimens made with high-alkali cement and cured in water, as shown in Figure 7. The presence of water had a relevant impact on the dissolution of the wool fibres in the alkaline environments. In the mortars stored for 3 days in water, wool fibres were still visible after cracking (Figure 7(a)), whereas in the mortars stored for 27 days in water, the wool fibres were completely dissolved (Figure 7(b)). In the latter, only empty holes in the cement matrix, having a diameter of about 20 μm, are visible. The chemical composition of the cement matrix around the holes was characterised by sulfur and potassium peaks, which can be attributed to the presence of wool fibres (see Figure 7).

In the room curing condition (27 days at 20°C and RH = 50%), the residual strength y_1 after cracking was nearly zero without any fibre reinforcement. As shown in Figure 8(a), for all types of cement, the reduction in strength of the plain mortar was greater than 95%. In the presence of fibre, a residual strength was clearly evident. Nevertheless, y_1 decreased with an increase in the alkalinity of the cement. Specifically, for the low-alkali cement, the contribution of the wool fibres is relevant, as the relative residual stress y_1 was about 0.3. With an increase in alkalinity, the wool becomes progressively less effective and y_1 reduced and nearly vanished in the case of high-alkali cement (<5%). Hence, the high-alkali cement produced the lowest contribution of y_1 (Figure 8(a)).

If left 27 days in water (at 20°C), the residual strength y_1 of the mortars containing fibres was more or less the same for all types of cement (see Figure 8(b)). The same trend (i.e. the higher the alkalinity, the lower y_1) can also be observed in Figure 8(c), where the values of y_1 measured in the fibre-reinforced specimens left for only 3 days in water at 20°C are reported. The values of y_1 are higher than those depicted in Figure 8(b), especially for the specimens made with low-alkali cement, whereas the average values of y_1 in H_3 (Figure 8(b)) and H_4 (Figure 8(c)) were more or less the same. In the micrographs, the effect of curing time in water is particularly visible in the mortar specimens made with wool fibres and high-alkali cement. If stored for only 3 days in water (Figure 9(a)), these mortars were characterised by partial degradation of the fibres, while for those stored for 27 days in the water, empty spots were present after the dissolution of fibres (Figure 9(b)).

In other words, the larger the pH and the longer the time of curing in water, the higher the degree of wool degradation and the lower the residual strength after cracking and the toughness of the wool-reinforced specimens. As a matter of fact, all the observations previously made for the relative residual strength y_1 can be extended to the area A_F (see Figure 10). Thus, if fibres are used to mitigate the effects of shrinkage, which affects cement-based structures a few days after casting, wool fibres can be effectively added to concrete mixtures, especially when both the alkalinity of the cement and the RH of the environment are low.

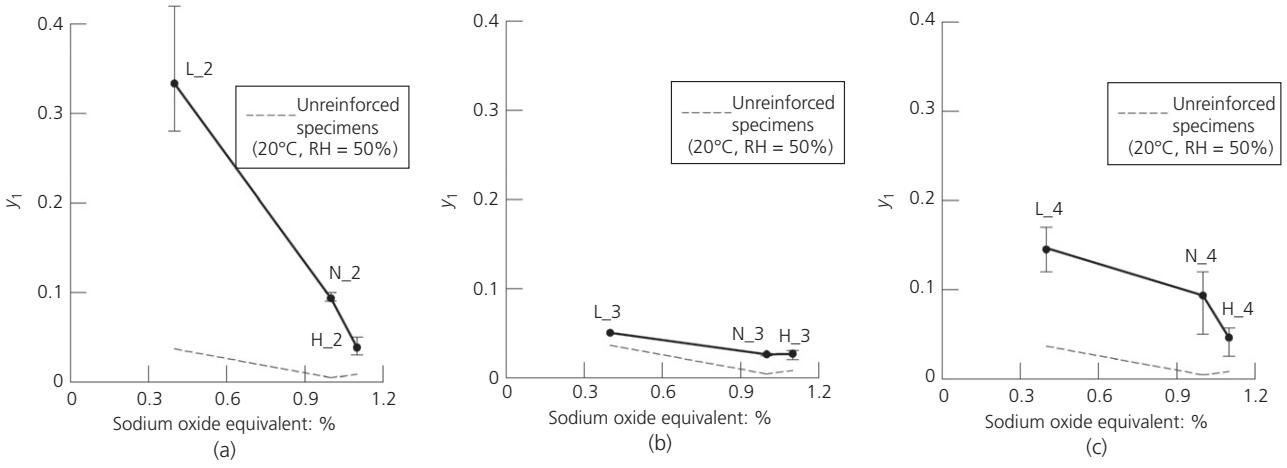

Figure 8. Residual stress y_1 measured in the three-point bending tests: (a) specimens cured for 27 days in room conditions (20°C, RH = 50%); (b) specimens cured for 27 days in water (20°C); (c) specimens cured for 3 days in water (20°C)

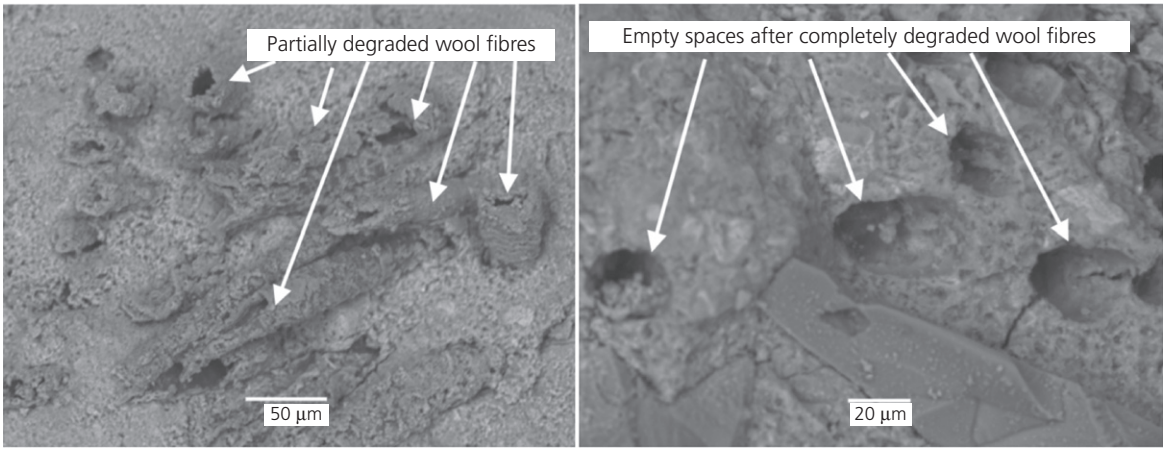

Figure 9. Microstructure of specimens made with high-alkali cement and addition of wool fibres after: (a) 3 days of curing in water at 20°C; (b) 27 days of curing in water at 20°C

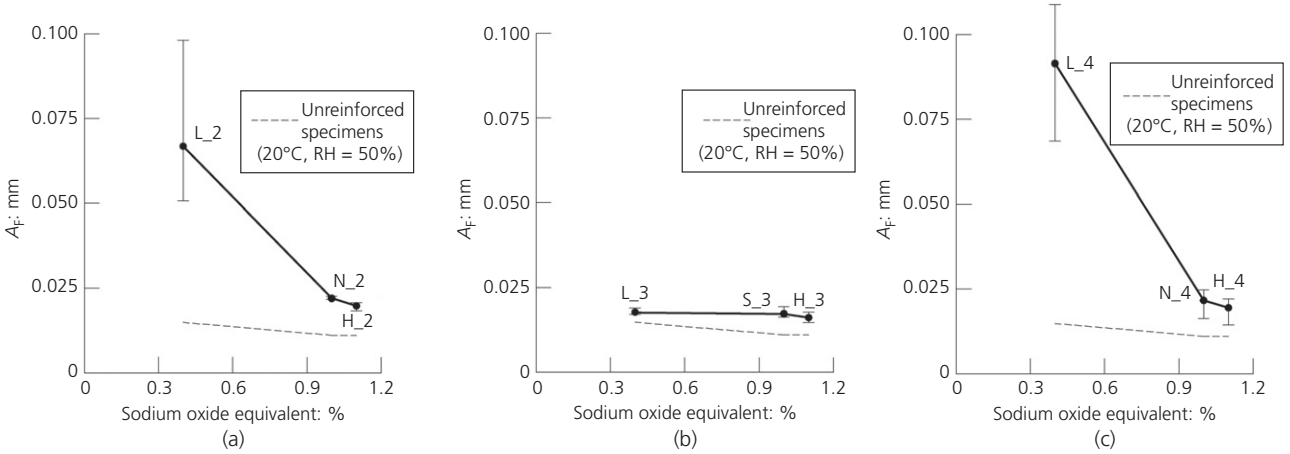

Figure 10. Area A_F measured in three-point bending tests: (a) specimens cured for 27 days in room conditions (20°C, RH = 50%); (b) specimens cured for 27 days in water (20°C); (c) specimens cured for 3 days in water (20°C)

5. Conclusions

From the results of the experimental tests performed on mortars made with different types of cement and reinforced with wool fibres, the following conclusions can be drawn.

- Flexural strength increases with the alkalinity of cement in plain mortars, but decreases in the case of wool reinforcement, due to reduced workability.
- The content of alkalis in the cement, as well as the curing time and curing method, have a strong influence on the microstructure of the mortars made with wool fibres. The higher the alkalinity and the time of curing in water, the higher the degree of wool fibre degradation. SEM analysis of the fracture surfaces revealed dissolution of the wool fibres and empty spaces corresponding to the size of wool fibres.
- Accordingly, the capability of wool fibres to bridge crack surfaces and to guarantee the presence of a residual tensile strength in the post-cracking stage reduces when high-alkali cement is used and in the presence of water. This was particularly highlighted by the values of the residual strength y_1 and the area A_F of the post-peak diagrams.

Future research studies will be devoted to comparing the residual strengths of cementitious mortars reinforced with wool with those containing polypropylene fibres.

Acknowledgement

The authors acknowledge the Italian Ministry of Education (PRIN 2015) for funding of this project.

REFERENCES

Allafi F, Hossain MS, Lalung J *et al.* (2020). Advancements in applications of natural wool fiber: review. *Journal of Natural Fibers* 1–16, https://doi.org/10.1080/15440478.2020.1745128.

BSI (2005) BS EN 196-1:2005: Methods of testing cement. Determination of strength. BSI, London, UK.

Fantilli AP, Vallini P and Chiaia B (2011) Ductility of fibre-reinforced self-consolidating concrete under multi-axial compression. *Cement & Concrete Composites* **33(4)**: 520–527.

Fantilli AP, Sicardi S and Dotti F (2017a) The use of wool as fibre-reinforcement in cement-based mortar. *Construction and Building Materials* **139**: 562–569.

Fantilli AP, Jóźwiak-Niedźwiedzka D, Gibas K and Dulnik J (2017b) The compatibility between wool fibres and cementitious mortars. In *Proceedings of the 2nd International Conference on Bio-Based Building Materials (ICBBM 2017)* (Amziane S and Sonebi M (eds)). RILEM Publications, Paris, France, pp. 42–47.

Fiore V, Di Bella G and Valenza A (2019) Effect of sheep wool fibers on thermal insulation and mechanical properties of cement-based composites. *Journal of Natural Fibers* 1–13, https://doi.org/10.1080/15440478.2019.1584075.

Giosué C, Mobili A, Yu QL *et al.* (2019) Properties of multifunctional lightweight mortars containing zeolite and natural fibers. *Journal of Sustainable Cement-Based Materials* **8(4)**: 214–227.

Grădinaru CM, Bărbuță M, Șerbănoiu AA and Babor D (2016) Investigations on the mechanical properties of concrete with sheep wool fibres and fly ash. *Bulletin of the Transilvania University of Braşov, Series I: Engineering Sciences* **9(58)**: 73–80.

Jena B, Mohanty BB and Sahoo K (2018) Comparative study on self-compacting concrete reinforced with different chopped fibres. *Proceedings of the Institution of Civil Engineers – Construction Materials* **171(2)**: 72–84, https://doi.org/10.1680/jcoma.16.00076.

Jóźwiak-Niedźwiedzka D and Fantilli AP (2017) Cement based composites with multifunctional addition of unused wool fibres. In *Energy Efficient, Sustainable Building Materials and Products* (Hager I (ed.)). Politechnika Krakowska, Krakow, Poland, pp. 267–282.

Jóźwiak-Niedźwiedzka D, Brandt AM and Ranachowski Z (2012) Self-healing of cracks in fibre reinforced mortar beams made with high calcium fly ash. *Cement Wapno Beton* **XVII/LXXIX(1)**: 38–49.

Pederneiras CM, Veiga R and de Brito J (2019) Rendering mortars reinforced with natural sheep's wool fibers. *Materials* **12(22)**: 3648–3660.

Ralegaonkar RV, Aswath PB and Abolmaali A (2019) Design investigations of basalt-fibre-reinforced mortar. *Proceedings of the Institution of Civil Engineers – Construction Materials* **172(6)**: 296–304, https://doi.org/10.1680/jcoma.17.00018.

Schokker AJ (2010) *The Sustainable Concrete Guide – Strategies and Examples.* U.S. Green Concrete Council, Farmington Hills, MI, USA.

Štirmer N, Milovanović B and Sokol JM (2014) Cement composites reinforced with sheep's wool. *Proceedings of the International Symposium on Eco-Crete* (Wallevik OH, Bager DH, Hjartarson B and Wallevik JE ((eds)). ICI Rheocenter, Reykjavik, Iceland, pp. 271–278.

Toledo Filho RD, Scrivener K, England GL and Ghavami K (2000) Durability of alkali-sensitive sisal and coconut fibres in cement mortar composites. *Cement & Concrete Composites* **22(2)**: 127–143.

Wei J and Meyer C (2014) Improving degradation resistance of sisal fibre in concrete through fibre surface treatment. *Applied Surface Science* **289**: 511–523, https://doi.org/10.1016/j.apsusc.2013.11.024.